Proceedings of the ASME 2014 International Design Engineering Technical Conferences & Computers and Information in Engineering Conference
IDETC/CIE 2014
August 17-20, 2014, Buffalo, New York, USA

DETC2014-35459

FINITE ELEMENT ANALYSIS WITHIN COMPONENT DESIGN PROCESS OF HYDRAULIC QUADRUPED ROBOT

Mariapaola D'Imperio
Istituto Italiano di Tecnologia
Department of Advanced Robotics
Genoa, Italy, 16163
Email: mariapaola.dimperio@iit.it

Ferdinando Cannella, Claudio Semini and D.G. Caldwell
Istituto Italiano di Tecnologia
Department of Advanced Robotics
Genoa, Italy, 16163
ferdinando.cannella@iit.it;
claudio.semini@iit.it;darwin.caldwell@iit.it

Daniele Catelani
MSC.Software srl
Torino, Italy, 10121
daniele.catelani@mscsoftware.com

Roberto Bernetti
Universita' Politecnica delle Marche
Ancona, Italy, 60121
rb@robertobernetti.com

ABSTRACT

The lightweight constructions and components stiffness play an important role in mechanics and in particular in high performance robots. In this paper the Virtual Prototyping Design (VPD) approach for addressing the robot design to this goal is shown. The VPD is applied to three mechanical problems of Walking Hydraulic Robots (WHRs): the first one deals with the leg joint sensitivity analysis; the second one concerns a force sensor optimization while the third one presents the torso structural verification. In all the aforementioned studies the experimental tests and the fitting analyses for model validation were carried out reaching satisfactory results.

NOMENCLATURE

A action body;
B reaction body;
i connection marker coordinate for A;
k connection marker coordinate for B;
i,k = x, y, z
E^A A position and orientation;
E^B B position and orientation;
d_i relative displacement between two bodies along i direction;
θ_i relative rotation between two bodies around i axes;
F_i translational force components acting on A;
F_k translational force components acting on B;
T_i torque component acting on A;
T_k torque component acting on B;
x,y,z rotational displacements of the i marker with respect to the k marker;
V_x, V_y, V_z time derivatives of x, y, and z;
F_1, F_2, F_3 constant force preload for B;
a,b,c rotational displacements of the i marker with respect to the k marker;
$\omega_x, \omega_y, \omega_z$ angular velocity of the i marker expressed in the k marker coordinate system;
T_1, T_2, T_3 constant torque preload for B;
K_{ij} stiffness matrix elements;
C_{ij} damping matrix elements.

INTRODUCTION

In the last decades, thanks to the improvement of the informatic technology, the application of Virtual Prototype Design (VPD) method in the robots development process is one of the most used ways to achieve the required optimum solution [1]. Different analysis domains, such as hybrid multibody system dynamics (MBS), finite element analysis (FEA), control system simulation and topology optimization are integrated into a straightforward way [2], [3], [4], [5], [6]. These promising techniques are applied to robotics successfully. It is also largely used for structural analysis [7], [8], and for simulating the kinematics and dynamics [9], [10], [11] [12]. However, these methods are not widely used to analyze the dynamics of walking robot hydraulic actuated.

The complexity of such robots makes it hard to improve the structural performance. The main issue is to maintain the tradeoff between the weight reduction and the structural strength. This can bring problems to the structural design and to the control methodology [16-17]. Decreasing the weight of the structure has two drawbacks. The first drawback is that it leads unwanted failures while the second one is the unwanted free vibrations generations which could disturb the control system [13], [14].

Walking Hydraulic Robots (WHRs) represent the most advanced robots with complex structure. This complex actuation system satisfies all the dynamic requests of WHRs because of its high power-to-weight ratio and high force capabilities. As example BigDog [15], Cheetah [16], KOLT [17] and LittleDog [18] are typical WHRs. Among the main problems related to these robots mechanical design, three of them are faced in this work: 1) the joint sensitivity analysis, 2) the compliance connection optimization process and 3) the structural component validation.

The first problem takes place at the early stage of the design process. It is linked to the bearings choice, whose stiffness governs the value of the internal forces. The second problem is related to the interaction between the actuation system and the feedback control for tuning the end effector applied torque. The third problem arises at the end of the physical prototyping process when the validation stage takes place.

The Hydraulic Quadruped HyQ [19], [20], [21], [22], [23], [24] (Fig.1-(a)) we are building is an example of WHR. That platform is designed to perform high dynamic tasks like jumping, running, climbing, etc. It is able to perform both indoor and outdoor operations like walking up to $2m/s$, jumping up to $0.5m$ and balancing the ground disturbance. HyQ weighs about $80kg$, is $1m$ long and $1m$ tall with fully stretched legs. Each HyQ' s leg (Fig.1-(b)) has 3 degrees of freedom (DOF): the hip and knee hydraulically actuated flexion/extension and the hip electrically actuated abduction/adduction. The maximum joint torque for both the hydraulic actuators is about $140Nm$.

The design process of HyQ structure finds the solution to the aforementioned as it happens for each WHR. The design of a new limb requires the choice of the bearings. At this stage the designer has to consider the stiffness of the whole structure, to avoid high stresses caused by rigid connections. The compliance joint estimation is an issue when HyQ is performing a motion on rough terrain. The validation process is also difficult to carry out because of its geometry complexity.

The aim of this paper is to show how Virtual Prototyping Design (VPD) can be applied to hydraulic robots design to solve all the aforementioned problems. In particular we are going to present three different applications for HyQ components. The first one deals with the joint sensitivity analysis of the leg in order to show how the connections stiffness can influence the forces in the structure. The second one concerns a compliance joint optimization where the goal is to determine the section size for obtaining the maximum signal for measuring. Third one is a structural verification that involves two different kinds of analyses: the static and dynamic for the torso. In all the aforementioned studies the experimental tests and the fitting analyses for model validation were carried out. The presented results will be assembled in a future stage in the full HyQ virtual prototype advanced structure.

The contributions of this work are the following: the application of the VPD to improve the performance of WHR thanks to a lightweight construction of some crucial components (leg, sensor and torso) and the exploitation of these models for the design the new release of the robots, saving physical prototypes building.

The rest of the paper is organized into four sections. Section *II* is a solution to Problem 1 about the joint sensitivity analysis: it contains the statement of the problem, the description of the numerical analysis and the discussion between the numerical and experimental results. Section *III* is a solution for Problem 2 about the compliance connection optimization process. Section *IV* is a solution to Problem 3 and it is referred to the structural component validation. Section *V* addresses the conclusions.

PROBLEM 1: JOINTS SENSITIVITY ANALYSIS

In this section we want to describe the advantages of using a good virtual prototype model in the bearing selection process in a robotic structure. The choice of connections, that affects the design since its early stage, is a tradeoff between mechanical and dynamical aspects.

The available space for the bearings, the axes misalignments, the issues linked to the assembly stage are always analyzed in a 3D CAD design.

All the problems referred to the link flexibility can be solved analytically or numerically. The first solution not only requires high mathematical skills but also time for reaching an optimum solution. The complexity increases exponentially with the degrees of freedom of the structure. To overpass the aforementioned issues the solution we propose is a simplified numerical model with lumped flexible connections. It is important to high-

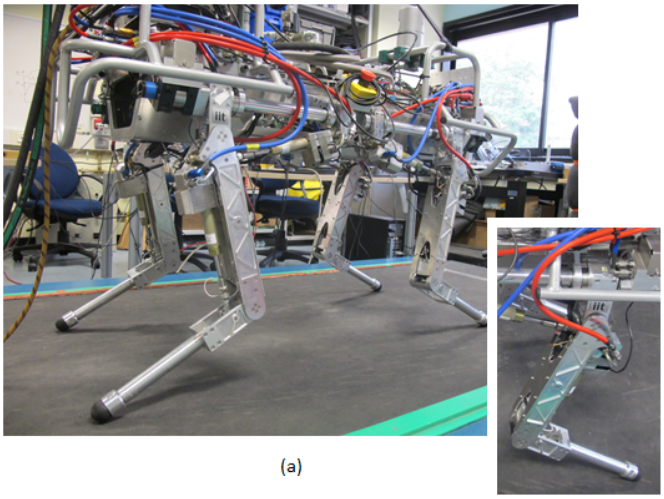

FIGURE 1. (a) HYQ HOLE STRUCTURE, (b) HYQ LEG

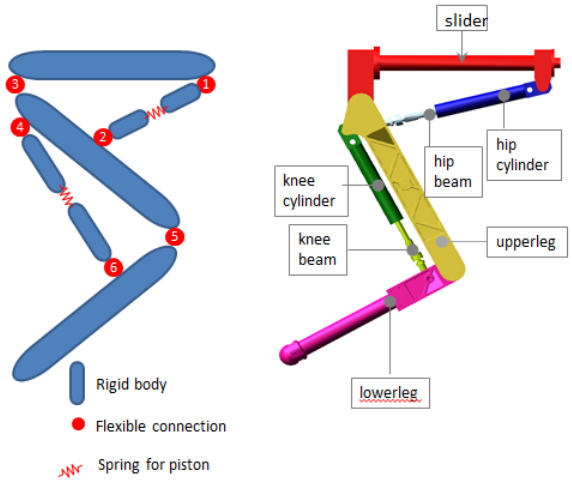

FIGURE 2. (a) SIMPLIFIED RIGID MULTIBODY MECHANISM WITH LUMPED FLEXIBLE CONNECTIONS, (b) HYQ LEG MULTIBODY SYSTEM.

light that the person who builds this model has to have an engineer background, in order to be able to accurately manipulate and manage the data. Once the numerical prototype is ready, also the designer can easily use it.

The importance of having a simplified model is due to the poor quantity of data available at the beginning of the design process, so it has no sense working with a complex model. With this solution, in fact, the modeling of the bodies flexibility is left to a second stage of the design, when the designer has a better and deep knowledge of the components.

In this paper the analysis was performed on one of the quadruped leg with the aim of investigating how much the connection stiffness is responsible of the reaction growing in the structure.

Numerical Model and Analysis

Each HyQ leg contains around 450 parts made by different materials: plastic for the electronics, oil for the hydraulics, steel and alloy for the mechanics. It means to have more than 2700 degrees of freedom. The physical leg, instead has only 2 degrees of freedom, it means that all the different components can be merged in several rigid bodies: one for each moving part of the structure [24].

A rigid body should be thought as an assembly of components that have no relative movements, whose behavior can be described referring at its center of the mass. The nature of each single component must be taken in account during the merging operation because the rigid assembly center of the mass position depends on the inertia of every single sub element.

At the end of the merging process for the HyQ leg 7 rigid bodies there were obtained: slider, upperleg, lowerleg, hip cylinder, hip beam, knee cylinder and knee beam (Fig. 2-(b)).

The model we present here, as already explained before, is a simplified rigid multibody mechanism with lumped flexible connections, whose schematic representation is shown in (Fig. 2-(a)).

The position of each single rigid body was characterized by three reference markers, two of these were placed at the ends of the body, on the ideal axis of connection with the adjacent part, the third one instead on the center of mass. The following step was the definition of the connections. Two different models were built: the one with the ideal connection was called RCP (Rigid Connected Prototype) while the one with flexible connection was called FCP (Flexible Connected Prototype), as explained in the further section. In each model, the actuators movement was modeled by using two spring-damping elements, whose characteristics depend on the oil and control properties.

Rigid Connected Prototype The connections in the RCP were based on the surface contact, they're usually defined as *lower pairs*. Considering two bodies A and B and the vectors that describe the position and rotation of each of them, the constraint law is represented by Eq. 2 (1) for the translations and 2 (2) for the rotations.

$$\mathbf{E}_i^A \cdot (\mathbf{u}^A - \mathbf{u}^B) - d_i = 0 \quad (1)$$

$$cos(\theta_i(\mathbf{E}_i^A \cdot \mathbf{E}_k^B)) - sin(\theta_i(\mathbf{E}_k^A \cdot \mathbf{E}_k^B)) = 0 \quad (2)$$

TABLE 1. DEFINITION OF THE SIX LOWER PAIRS JOINTS PROPERTIES.

	Relative displacement			Relative rotation		
Joint type	d_1	d_2	d_3	θ_1	θ_2	θ_3
Revolute	0	0	0	0	0	$\neq 0$
Prismatic	0	0	$\neq 0$	0	0	0
Screw	0	0	$p\theta_3$	0	0	$\neq 0$
Cylindrical	0	0	$\neq 0$	0	0	$\neq 0$
Planar	$\neq 0$	$\neq 0$	0	0	0	$\neq 0$
Spherical	0	0	0	$\neq 0$	$\neq 0$	$\neq 0$

The scenario of rigid connections is composed by six different joints, whose properties are summarized in Tab. 1. These are mostly ideal connections that serve to evaluate the kinematics of the mechanism.

In the HyQ leg RCP model the chosen connections were mostly *cylindrical*, because the actuators is assigned to a spring-damper element as aforementioned before.

Flexible Connected Prototype The connections in the FCP were modeled by using the *bushing* element among the choice offered by MSC Adams. The bushings apply a force on the reaction body that could be expressed by Eq.3.

$$F_k = -F_i \tag{3}$$

$$T_k = -Ti - \delta \cdot F_i \tag{4}$$

The constitutive law for each connection is described the Eq. 5.

$$\begin{bmatrix} F_x^A \\ F_y^A \\ F_z^A \\ T_x^A \\ T_y^A \\ T_z^A \end{bmatrix} = - \begin{bmatrix} K_{11} & 0 & 0 & 0 & 0 & 0 \\ 0 & K_{22} & 0 & 0 & 0 & 0 \\ 0 & 0 & K_{33} & 0 & 0 & 0 \\ 0 & 0 & 0 & K_{44} & 0 & 0 \\ 0 & 0 & 0 & 0 & K_{55} & 0 \\ 0 & 0 & 0 & 0 & 0 & K_{66} \end{bmatrix} \begin{bmatrix} x \\ y \\ z \\ a \\ b \\ c \end{bmatrix} + \begin{bmatrix} C_{11} & 0 & 0 & 0 & 0 & 0 \\ 0 & C_{22} & 0 & 0 & 0 & 0 \\ 0 & 0 & C_{33} & 0 & 0 & 0 \\ 0 & 0 & 0 & C_{44} & 0 & 0 \\ 0 & 0 & 0 & 0 & C_{55} & 0 \\ 0 & 0 & 0 & 0 & 0 & C_{66} \end{bmatrix} \begin{bmatrix} V_x \\ V_y \\ V_z \\ \omega_x \\ \omega_y \\ \omega_z \end{bmatrix} + \begin{bmatrix} V_x \\ V_y \\ V_z \\ \omega_x \\ \omega_y \\ \omega_z \end{bmatrix} \tag{5}$$

For a complex modeling it is possible to use a *field* connection that has all the terms K_{ij} and $C_{ij} \neq 0$. That choice involves the deep knowledge of the bearings that the designer intend to model, this aspect is beyond the scope of paper.

In both of cases we performed a drop test analysis with the aim to investigate the leg dynamics. In the numerical model we reproduced the same test we've done on the physical leg and described in the following section. The first analysis was carried out on the RCP model; the second one on a FCP with 4 bushings (that correspond to bushings number 1,2,3,6 of Fig.2-(a); at last the third analysis was done using a FCP model with 8 bushings (that correspond to bushings number 1,2,3,4,5,6 of Fig.2-(a).

The results from all of the aforementioned analysis were mainly the forces in the hip and knee pistons and the slider vertical displacement. All these data were compared with the measurements coming from an exhaustive campaign of experimental tests done with the physical leg.

Experimental Tests

The experimental drop test of one of the HyQ leg is here presented. The leg at the beginning of the test was standing, in its equilibrium position. In a second stage it was left up to reach a fixed elevation, after it was dropped down and then left free to oscillate until the end of vibrations due to the impact. The test vertical alignment was guaranteed by a low frictional sleeve fixed on a vertical guide. The experiment was repeated three times for each chosen height in order to have statistically valid data. The measured quantities were the slider position (*Absolute Encoder austriamicrosystem AS5045, signal 12Bit, resolution 0.0879deg*) and the forces on the load cells (*Burster 8417, force range 0-5 kN, accuracy 0.5 %*). The positions of the aforementioned instruments is shown in Fig.3.

Discussion

The comparison between the RCP model and experimental tests data shows that it is possible to reach an agreement only between the numerical and physical slider displacement (Fig.4). The forces that grow up in the numerical model, in fact, as expected are higher than the one registered on the physical leg (Fig.5 and Fig.6), cause of the high stiffness of the all structure.

The rigid joints are ideal connections with infinitive stiffness, the physical one instead has a finite value of stiffness. As shown in the results of the FCP models, in fact, the agreement between the numerical and experimental values gives satisfactory results. In both of cases the matching between numerical and experimental displacement was reached (Fig.7 and Fig.10).

The model with 4 bushings affects only the results for the hip force (Fig.8 and Fig. 9) because its behavior mostly depends

[0]Consider that the bushings n4 and n5 respectively are double because in these cases the connection has two sides.

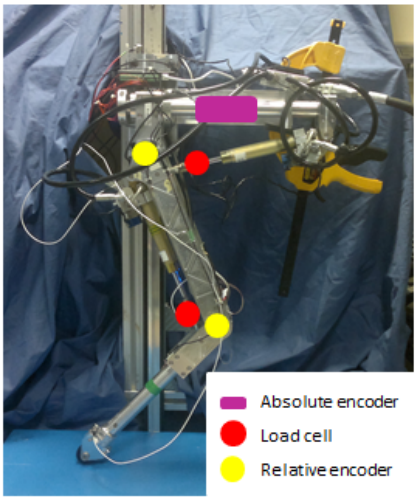

FIGURE 3. INSTRUMENTED HYQ LEG.

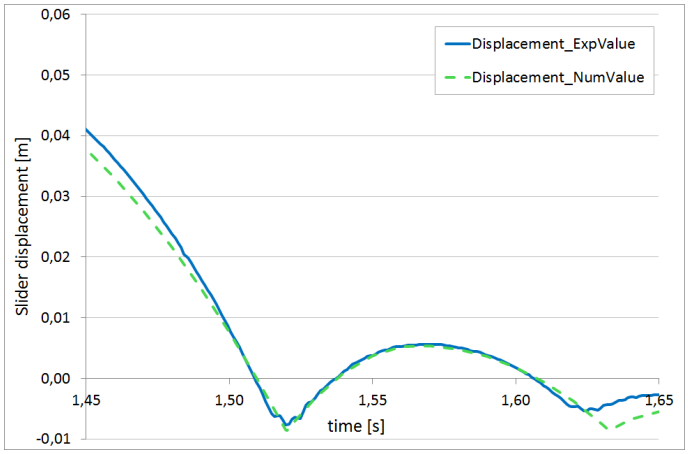

FIGURE 4. RCP SLIDER DISPLACEMENT COMPARISON.

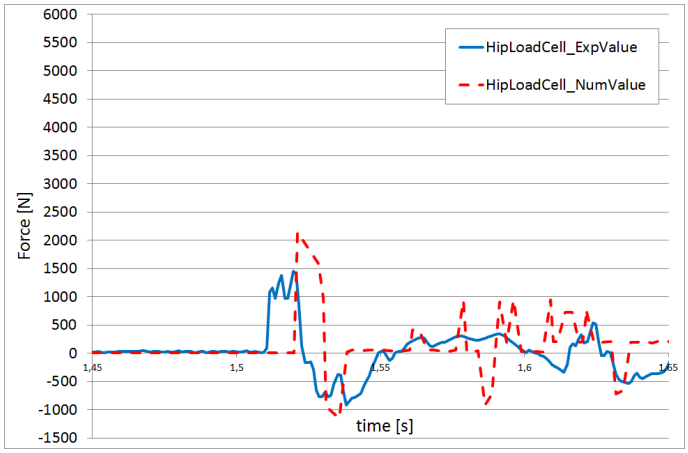

FIGURE 5. RCP HIP FORCE COMPARISON.

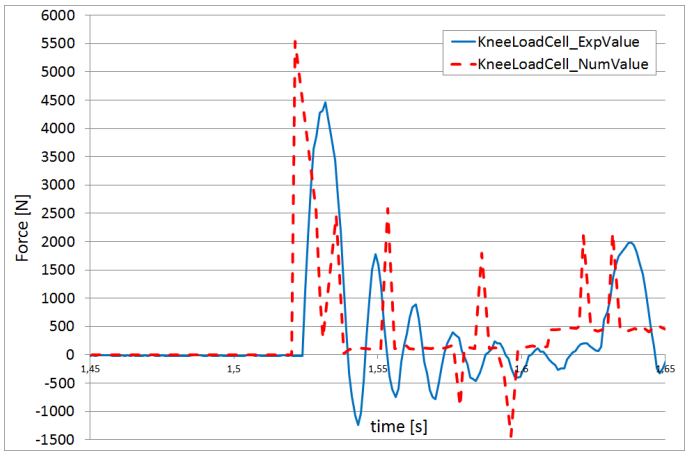

FIGURE 6. RCP KNEE FORCE COMPARISON.

on the flexibility of the connection pins between this structure and the mechanical component, upperleg from one side, slider from the other one.

The model built with using 8 bushings, instead, reaches the agreement for both the load cells (Fig.11 and Fig.12). In this case the matching with the knee results was obtained because the movement of the knee actuator depends not only by the flexibility of the connection pins with the upperleg and lowerleg, but also on the stiffness of the connections between these two mechanical parts.

PROBLEM 2: COMPLIANCE CONNECTION OPTIMIZATION PROCESS

The second case study we want to present in this paper is the application of the VPD to the complete design process of a torque sensor [25]. Nowadays the control force is undergoing a rapid development, it is moving away from the rigid joint to look forward to the design of fully sensorized joints based on the applications of torque sensors. Generally, in a force control loop, these ones allow the motor to tune the torque applied to the end effector.

There are several reasons which have prompted this improvement. The application of flexible joints makes safer the hand to hand collaboration between robots and humans, allows the storage of the energy due to an impact for avoiding structural damages, increases the precision in a manufacturing process.

The solution presented, thus, is a new optimized torque sensor design that not only fits perfectly with the current mechanism assembly, but also guarantees the required mechanical properties of the joint. The use of the VPD technique allows the possibility of test several solutions before reaching the final one.

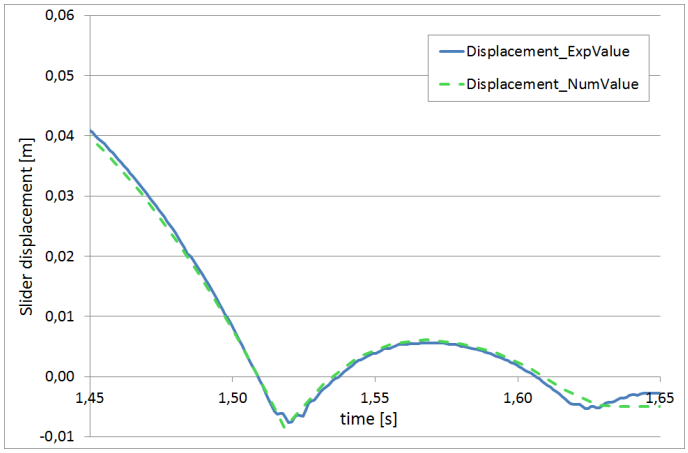

FIGURE 7. FOUR BUSHINGS FCP SLIDER DISPLACEMENT COMPARISON.

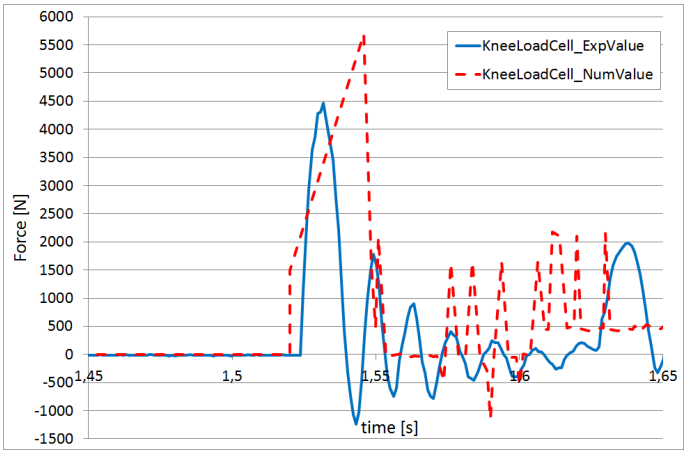

FIGURE 9. FOUR BUSHINGS FCP KNEE FORCE COMPARISON.

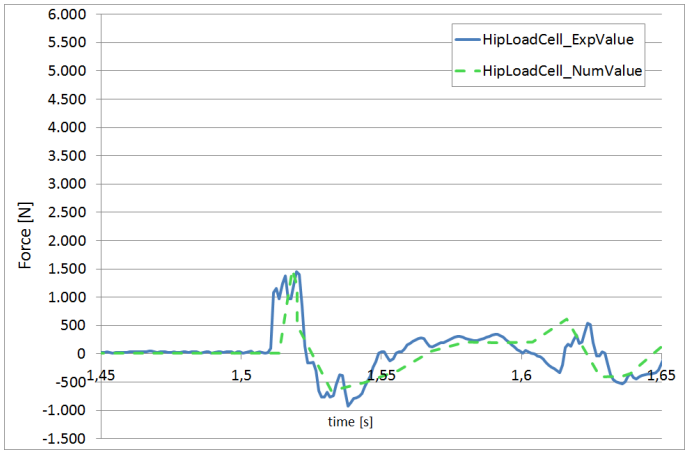

FIGURE 8. FOUR BUSHINGS FCP HIP FORCE COMPARISON.

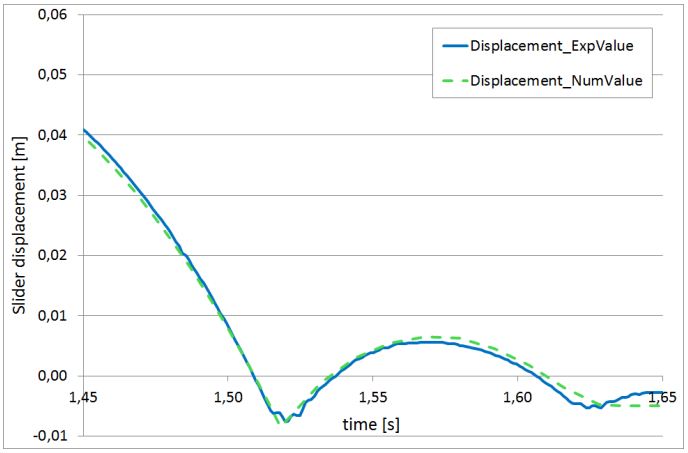

FIGURE 10. EIGHT BUSHINGS FCP SLIDER DISPLACEMENT COMPARISON.

Numerical Model and Analysis

The structure presented was a 1 degree of freedom (DOF) torque sensor whose deformations are estimated by positioning strain gauges. The solid was meshed by using a 3D tetrahedral element that exhibits quadratic displacement behavior. The element supports plasticity, large deflection and large strain capabilities. The specifications imposed to use Ergal as building material.

The design boundary conditions, as happen for each measurement tool, depend on the admissible stiffness k ($k = \frac{torque}{deg}$) and on the measurement technique chosen.

That first one can influence the reaction time of the control system: the decrement of the stiffness induces a loss in the system accuracy. In the case presented, the maximum dynamic torque transmitted by the motor was around $140Nm$ and the related angle is around $1deg$.

The second one is represented by the strain gauges applications. That technique is based on the principle of the local deformation. It means that it is important to concentrate the maximum strain of the body in a specific area, where the sensors will be positioned. This value, lower than 0.06%, produces a suitable input for the strain gauge within the linearity that is 0.15%. The aforementioned surface must be accessible and planar.

The accessibility is useful to guarantee the correct positioning of the sensor, whose procedure requires the cleaning of the surface, the bondage of the film gluing and of the cables wiring. The planarity, instead, is important to avoid offset and drift phenomena that can arise in case of curved surfaces.

The leg movement can be both in the clockwise direction and in count clockwise, for this reason it should be better having the same calibration factor in both directions. That will guarantee an easy integration of the structure in the control system.

The final shape of the structure was obtained by an opti-

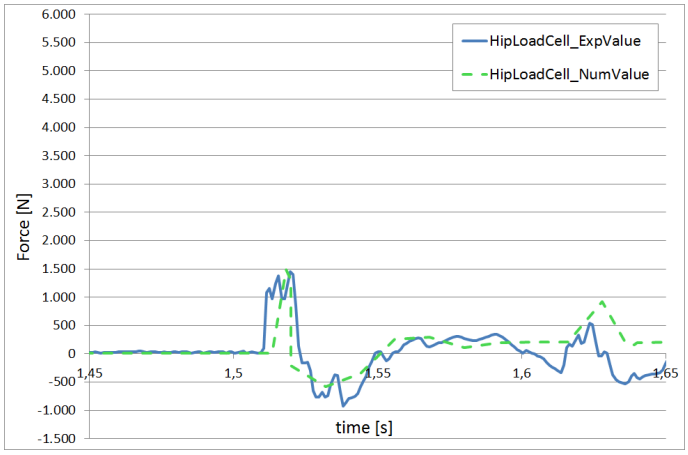

FIGURE 11. EIGHT BUSHINGS FCP HIP FORCE COMPARISON.

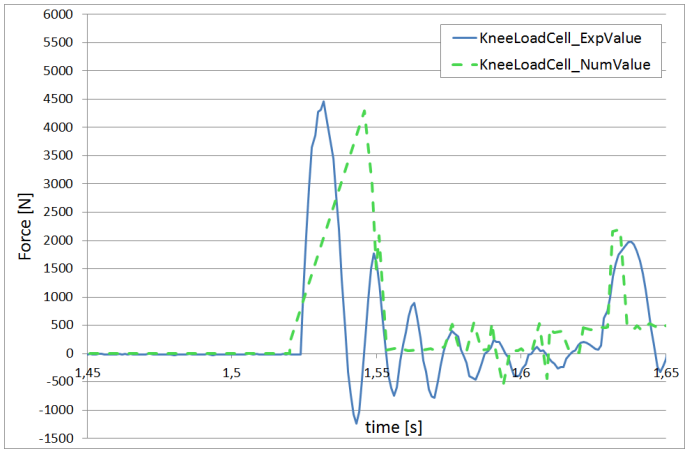

FIGURE 12. EIGHT BUSHINGS FCP KNEE FORCE COMPARISON.

mization process divided in four case studies. Every single case study was composed by two different steps: the initial shape was obtained according to the applied design rule; then it was optimized thanks to ModeFRONTIER simulations, in order to determine the best performances. This procedure was looped till these performances matched the torque sensor requirements.

As it is obvious, the torsion is the basic phenomenon of torque sensor concept. That leads to think that the circular shape can produce the maximum deformation in safe conditions. Thus the first idea would have been to design a hollow cylinder to be installed between the harmonic drive and the shaft motor. However, in this way, it was not possible to match the requested deformation. Then other designs were investigated and all the structural capabilities of each solution were tested by numeric simulation developed in MSC Nastran. Two different constraint conditions were tested, to simulate the reciprocal displacement between the two sides. In the first case the torque sensor is fixed to the harmonic drive and the torque is applied by the shaft motor; the second one, instead, is the inverse.

Discussion

Based on the aforementioned criteria, the first solution investigated is shown in Fig.13-(a). The maximum stress, that arose close to the connection between the inner circular section and the linear beam, exceeded the yield point of the material. The area where the maximum strain was located was not planar and the reached value of deformation was not sufficient for the strain gauges measurement. However that shape guaranteed a bidirectional behavior. Considering that this solution did not match several requested specifications, it was abandoned.

The second structure has been designed keeping a similar shape of the former one but more robust. It was composed by two cylindrical concentric bodies linked each other by four rectangular components. Despite that improving, some problems of the previous solution still existed. The only one solved was the deformation value, it was within the measurement range of the strain gauges. At the end, even this second solution was deleted.

The shape of the third solution has followed the torsional flow stress: the link between the two cylindrical bodies was obtained by deformable components subjected only a tensile stress because they were put tangentially to the flow stress. The structure was more robust than the previous cases in order to guarantee the elastic response of the body. The deformable components, the two horizontal links, were subjected to a pure tensile stress. The strain was bigger than the previous times and allowed the reaching of the design specifications. The robustness allowed to remain in the elastic field of the material. However, even if the positioning strain gauges surfaces were planar, they were inaccessible for film bondage and the cable working space.

The last solution investigated, grew up from the failures of the previous one (Fig.13-(b)). The robustness and the idea to get the deformation thanks to a pure tensile stress were saved. The main work was focused in the increase of the empty space close o the planar surface to guarantee a successful strain gauges position. That solution covered almost everyone the required tasks. The exception was represented by the bi-directionality. To solve this problem, the suggested solution was to use two different calibration factors according to the clockwise or anti-clockwise movement.

Problem 3: STRUCTURAL COMPONENT VALIDATION

The verification process of the HyQ torso is here presented. It was based on a comparative modal analysis results between the numerical model and the physical one. The choice of using such analysis was due to the nature of the body and to the possibility of using the results even for further structural considerations. The

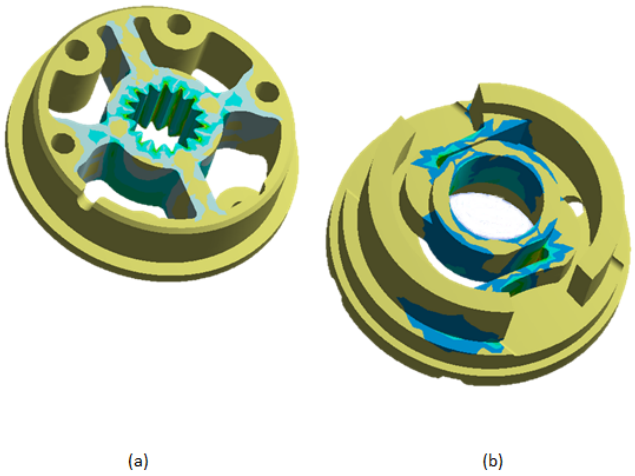

FIGURE 13. 1 DOF TORQUE SENSOR SOLUTIONS: (a) FIRST, (b) LAST.

torso is a rigid body, so the modal analysis was the easiest way to determine the dynamic properties of the physical structure. As second reason, these results can give an estimation on the distance between the torso natural frequencies and the ones of legged robots typical movements like walk, trot, run or gallop. [26]

Numerical Model and Analysis

The VPD, built using tetrahedral elements, was subjected to a modal analysis [26]. The results, shown in Tab.2 and Fig.15 show that the lower frequencies influence the behavior of the heavy masses of the structure as electrical motor, pump and the tank, as shown in Fig.15-(a) and Fig.15-(b); the higher frequencies are more related to the torso structure, as shown in Fig.15-(c) and Fig.15-(d). The natural modes shape of the remaining body are located in the range of the higher frequencies. This is due to the ratio between bodies masses and stiffness.

Experimental tests

During this campaign of experiment the torso, instrumented by accelerometers (*Dytran 3097A3, frequency range 0.3-5 Hz , accuracy 5 %*) set in several key positions, was leaned on a soft material (Fig.14). The measurements were carried out giving a hammer impulse as input to the structure and recording the accelerometer signal as outputs. All the data were acquired via PC and the spectrum analyzer permitted to check the result in real time.

Discussion

The mainly result of the modal analysis on the torso is the agreement between the frequencies of the experimental model and the numerical one (Tab.2). The numerical frequencies are not so far from the real ones, it allows to consider the numerical model like a good representation of reality and permits to have an instrument for further design of the torso in order to obtain a lighter or stronger structure without prototyping it.

TABLE 2. COMPARISON BETWEEN NUMERICAL AND EXPERIMENTAL ANALYSIS.

Numerical [Hz]	Experimental [Hz]	Difference
1.8	2	10%
32	30	6%
40	37	8%
120	112	7%
143	145	1.3%
152	155	1.3%

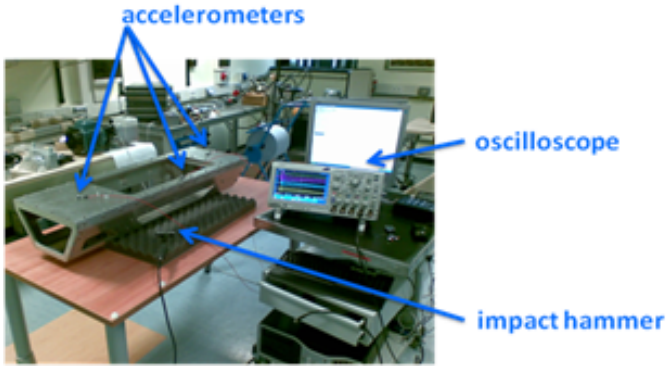

FIGURE 14. EXPERIMENTAL TEST.

CONCLUSIONS

In this work it is presented the VPD applied to a high performance quadruped robot: HyQ (Hydraulically Quadruped). Thanks to a lightweight construction of some crucial components the structure and the sensors were improved. In particular the leg joints, the torque sensor and the torso were modeled and validated in order to deeply investigate the mechanical behavior. That permitted to design the components that fit as much as closer with the robot requirements in terms of weight, stiffness and sensitivity. Moreover the obtained numerical models will be exploited for simulating the performance of the new releases of the HyQ without any further experimental tests.

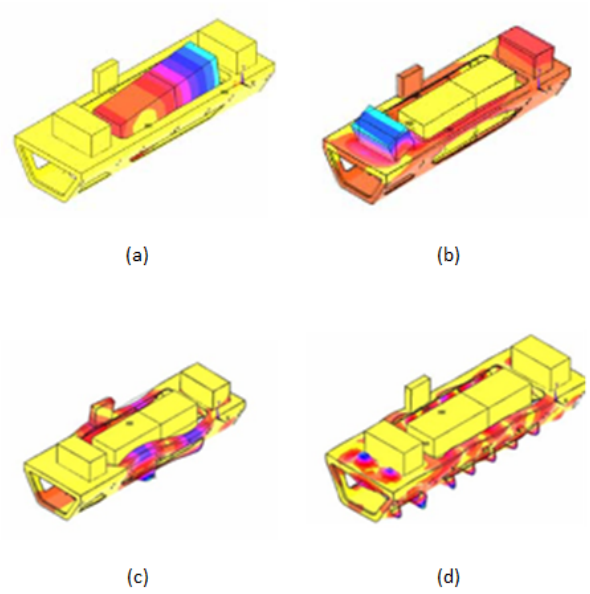

FIGURE 15. HEAVY MASSES MODE SHAPE (a) 1.8 Hz, (b) 8.7 Hz. TORSO STRUCTURE MODE SHAPE (c) 145 Hz, (d) 152 Hz.

ACKNOWLEDGMENT

The authors gratefully acknowledge Fei Chen and Mariacarla Memeo for the support.

REFERENCES

[1] O.C. Zeinkiewicz, R. T., and Zhu, J., 2005. *The Finite Element Method: Its Basis and Fundamentals.*, Vol. 6th edition.

[2] Kübler, R., and Schiehlen, W., 2000. "Modular simulation in multibody system dynamics". *Multibody System Dynamics,* ***4***(2-3), pp. 107–127.

[3] Ortiz, J., and Bir, G., 2006. "Verification of new msc adams linearization capability for wind turbine applications". In 44th AIAA Aerospace Sciences Meeting and Exhibit, Reno, Nevada.

[4] Cha H., Yun D., R. S. L. S., 2007. "Development of paper feeding control system using co-simulations tool". *Proceedings of the ASME 2007 International Design Conference & Computers and Information in Engineering Conference IDECT/CIE*, September 4-7. Las Vegas, Nevada, USA.

[5] Hoshino H., S. M., 2007. "Structural optimization in multibody dynamics system with finite element model on engine components". *Proceedings*, September 4-7. Las Vegas, Nevada, USA@articlekroll2011lightweight, title=Lightweight components for energy-efficient machine tools, author=Kroll, Lothar and Blau, Peter and Wabner, Markus and Frieß, Uwe and Eulitz, Jan and Klärner, Matthias, journal=CIRP Journal of Manufacturing Science and Technology, volume=4, number=2, pages=148–160, year=2011, publisher=Elsevier @articlekroll2011lightweight, title=Lightweight components for energy-efficient machine tools, author=Kroll, Lothar and Blau, Peter and Wabner, Markus and Frieß, Uwe and Eulitz, Jan and Klärner, Matthias, journal=CIRP Journal of Manufacturing Science and Technology, volume=4, number=2, pages=148–160, year=2011, publisher=Elsevier .

[6] Kroll, L., Blau, P., Wabner, M., Frieß, U., Eulitz, J., and Klärner, M., 2011. "Lightweight components for energy-efficient machine tools". *CIRP Journal of Manufacturing Science and Technology,* ***4***(2), pp. 148–160.

[7] Bayo, E., 1987. "A finite-element approach to control the end-point motion of a single-link flexible robot". *Journal of Robotic Systems,* ***4***(1), pp. 63–75.

[8] Diddens, D., Reynaerts, D., and Van Brussel, H., 1995. "Design of a ring-shaped three-axis micro force/torque sensor". *Sensors and Actuators A: Physical,* ***46***(1), pp. 225–232.

[9] Vaculín, O., Krüger, W. R., and Valášek, M., 2004. "Overview of coupling of multibody and control engineering tools". *Vehicle System Dynamics,* ***41***(5), pp. 415–429.

[10] Park, J.-H., and Asada, H., 1993. "Concurrent design optimization of mechanical structure and control for high speed robots". In American Control Conference, 1993, IEEE, pp. 2673–2679.

[11] Albers, A., Ottnad, J., Weiler, H., and Häussler, P., 2007. "Methods for lightweight design of mechanical components in humanoid robots". In Humanoid Robots, 2007 7th IEEE-RAS International Conference on, IEEE, pp. 609–615.

[12] Li Wang, E. G. Z., 2014. "Kinematic simulation and structural optimization analysis of some kind of transfer robot". *Applied Mechanics and Materials*, January.

[13] Ghiorghe, A., 2010. "Optimization design for the structure of an rrr type in ro". *U.P.B. Sci. Bull.*

[14] Sander, C., Yang, T., and Albers, A. "Design for energy efficiency: New structural optimization process for a robot shifter".

[15] Wooden, D., Malchano, M., Blankespoor, K., Howardy, A., Rizzi, A. A., and Raibert, M., 2010. "Autonomous navigation for bigdog". In Robotics and Automation (ICRA), 2010 IEEE International Conference on, IEEE, pp. 4736–4741.

[16] Wang, X., Li, M., Guo, W., Wang, P., and Sun, L., 2012. "Design and development of a cheetah robot under the neural mechanism controlling the leg's muscles". In Intelligent Robots and Systems (IROS), 2012 IEEE/RSJ International Conference on, IEEE, pp. 2749–2755.

[17] Cho, S.-H., 2012. "Cae services on cloud computing plat-

form in south korea". In *AsiaSim 2012*. Springer, pp. 440–446.

[18] Murphy, M. P., Saunders, A., Moreira, C., Rizzi, A. A., and Raibert, M., 2011. "The littledog robot". *The International Journal of Robotics Research,* ***30***(2), pp. 145–149.

[19] Semini, C., Tsagarakis, N. G., Vanderborght, B., Yang, Y., and Caldwell, D. G., 2008. "Hyq-hydraulically actuated quadruped robot: Hopping leg prototype". In Biomedical Robotics and Biomechatronics, 2008. BioRob 2008. 2nd IEEE RAS & EMBS International Conference on, IEEE, pp. 593–599.

[20] Semini, C., Tsagarakis, N. G., Guglielmino, E., Focchi, M., Cannella, F., and Caldwell, D. G., 2011. "Design of hyq–a hydraulically and electrically actuated quadruped robot". *Proceedings of the Institution of Mechanical Engineers, Part I: Journal of Systems and Control Engineering,* ***225***(6), pp. 831–849.

[21] Havoutis, I., Semini, C., and Caldwell, D., 2012. "Progress in quadrupedal trotting with active compliance". *Dynamic Walking*.

[22] Boaventura, T., Focchi, M., Frigerio, M., Buchli, J., Semini, C., Medrano-Cerda, G. A., and Caldwell, D. G., 2012. "On the role of load motion compensation in high-performance force control". In Intelligent Robots and Systems (IROS), 2012 IEEE/RSJ International Conference on, IEEE, pp. 4066–4071.

[23] Guglielmino, E., Cannella, F., Semini, C., Caldwell, D. G., Rodríguez, N. E. N., and Vidal, G., 2010. "A vibration study of a hydraulically-actuated legged machine". ASME.

[24] Yang, Y., Semini, C., Tsagarakis, N. G., Guglielmino, E., and Caldwell, D. G., 2009. "Leg mechanisms for hydraulically actuated robots". In Intelligent Robots and Systems, 2009. IROS 2009. IEEE/RSJ International Conference on, IEEE, pp. 4669–4675.

[25] M. D'Imperio, F. Cannella, J. G. C. S., and Caldwell, D., 2013. "Advanced shape for robotic torque sensor". *Newsletter Enginsoft*, December.

[26] Guglielmino, E., Cannella, F., Semini, C., Caldwell, D. G., Rodríguez, N. E. N., and Vidal, G., 2010. "A vibration study of a hydraulically-actuated legged machine". ASME.